Published in final edited form as:

*J Neurochem*. 2016 October ; 139(1): 96–105. doi:10.1111/jnc.13751.

# Deficiency in the voltage-gated proton channel Hv1 increases M2 polarization of microglia and attenuates brain damage from photothrombotic ischemic stroke

**Dai-Shi Tian**[1], **Chun-Yu Li**[1], **Chuan Qin**[1], **Madhuvika Murugan**[2], **Long-Jun Wu**[2,#], and **Jun-Li Liu**[3,#]

[1]Department of Neurology, Tongji Hospital, Tongji Medical College, Huazhong University of Science and Technology, Wuhan 430030, China

[2]Department of Cell Biology and Neuroscience, Rutgers University, Piscataway, NJ 08854

[3]Cancer center, Union Hospital, Tongji Medical College, Huazhong University of Science and Technology, Wuhan 430022, China

## Abstract

Microglia become activated during cerebral ischemia and exert pro-inflammatory or anti-inflammatory role dependent of microglial polarization. NADPH oxidase (NOX)-dependent reactive oxygen species (ROS) production in microglia plays an important role in neuronal damage after ischemic stroke. Recently, NOX and ROS are consistently reported to participate in the microglial activation and polarization; NOX2 inhibition or suppression of ROS production are shown to shift the microglial polarization from M1 toward M2 state after stroke. The voltage-gated proton channel, Hv1, is selectively expressed in microglia and is required for NOX-dependent ROS generation in the brain. However, the effect of Hv1 proton channel on microglial M1/M2 polarization state after cerebral ischemia remains unknown. In the present study, we investigated the role of microglial Hv1 proton channel in modulating microglial M1/M2 polarization during the pathogenesis of ischemic cerebral injury using a mouse model of photothrombosis. Following photothrombotic ischemic stroke, wild-type mice presented obvious brain infarct, neuronal damage and impaired motor coordination. However, mice lacking Hv1 ($Hv1^{-/-}$) were partially protected from brain damage and motor deficits compared to wild-type mice. These rescued phenotypes in $Hv1^{-/-}$mice in ischemic stroke is accompanied by reduced ROS production, shifted the microglial polarization from M1 to M2 state. Hv1 deficiency was also found to shift the M1/M2 polarization in primary cultured microglia. Our study suggests that the microglial Hv1 proton channel is a unique target for modulation of microglial M1/M2 polarization in the pathogenesis of ischemic stroke.

[#]**Correspondence to:** Dr. Long-Jun Wu, Dept. of Cell Biology and Neuroscience, Rutgers University, 604 Allison Road, Piscataway, NJ 08854, TEL: (848) 445-2182; FAX: (732) 445-5870, lwu@dls.rutgers.edu, OR Dr. Jun-Li Liu, Cancer center, Union Hospital, Tongji Medical College, Huazhong University of Science and Technology, Wuhan 430022, China, junli78@foxmail.com.

ARRIVE guidelines have been followed:

Yes => if No, skip complete sentence => if Yes, insert “All experiments were conducted in compliance with the ARRIVE guidelines.”

conflict of interest disclosure

The authors have no conflict of interest to declare.

**Keywords**

Voltage-gated proton channel Hv1; Microglia; Polarization; Ischemic stroke; Photothrombosis

## Introduction

Ischemic stroke is characterized by the sudden loss of blood circulation to an area of the brain, resulting in a corresponding loss of neurological function. During the ischemic process, reactive oxygen species (ROS) are produced which trigger apoptotic pathways, accompanied by microglial activation and inflammatory response (Hur *et al.* 2010). Inflammation-associated oxidative burst in activated microglia and macrophages is considered to be the major source of ROS in ischemic stroke (Miller *et al.* 2013). NADPH oxidase (NOX) is a membrane–bound enzyme that is abundantly expressed in phagocytic cells, including microglia (Wu *et al.* 2012) (Cooney *et al.* 2013). Indeed, NOX-dependent ROS production in inflammatory cells plays an important role in neuronal apoptosis and free radical-mediated tissue injury in the pathogenesis of cerebral ischemia (Kahles *et al.* 2010; Kahles *et al.* 2007).

Traditionally, microglia activation is considered to play a deleterious role in ischemic stroke since inhibition of microglia activation attenuates ischemic brain injury (Yrjänheikki *et al.* 1998). However, increasing evidence show that microglia activation is critical for attenuating neuronal apoptosis, enhancing neurogenesis, and promoting functional recovery after cerebral ischemia (Taylor and Sansing 2013; Hu *et al.* 2012). The biphasic role of microglia could be due to their polarization along a continuum from a classical pro-inflammatory M1-like state to an alternative anti-inflammatory M2-like state (Ma *et al.* 2016). Recently, NOX and ROS are consistently reported to participate in the microglial activation and polarization after brain infarction or injury; NOX2 inhibition altered M1-/M2-like balance in favor of the anti-inflammatory M2-like phenotype, and significantly reduced oxidative damage in neurons post-injury (Kumar *et al.* 2015). Similarly, suppression of ROS production shifted the microglial polarization from M1 toward M2 state, and attenuated brain injury after stroke (Choi *et al.* 2012).

Hv1 (encoded by gene *Hvcn1*), a novel voltage-gated proton channel, plays an important role in charge compensation for NOX activation by sensing both voltage and pH gradients, and deletion or inhibition of Hv1 greatly reduces NOX- dependent ROS production (Wu 2014b; Ramsey *et al.* 2006; Sasaki *et al.* 2006). Recently, we identified that Hv1 was selectively expressed in microglia and was required for NOX-dependent ROS generation in the brain(Wu *et al.* 2012). In addition, we found that mice lacking Hv1 ($Hv1^{-/-}$) were protected from NOX-mediated neuronal death and brain damage after ischemic stroke (Wu *et al.* 2012) or from NOX-dependent injury in cuprizone-induced demyelination (Liu *et al.* 2015). However, besides controlling NOX-dependent ROS production, whether Hv1 deletion could ameliorate neuronal damage by modulation of microglia polarization in ischemic stroke remains to be elucidated.

In the present study, we investigated the role of microglial Hv1 proton channel in ROS induced-neuronal damage in photothrombotic ischemic stroke. In particular, we tested

whether Hv1 is a potential target for modulating microglial M1/M2 polarization in the pathogenesis of ischemic cerebral injury.

## Methods and Materials

### Photothrombotic Cortical Ischemia

Male mice including wild-type (WT) C57BL/6 mice and $Hv1^{-/-}$mice were used in the present study. All mice were provided by Laboratory Animal Facilities of Hubei Center(Wuhan, China) or Jax laboratory (USA) except $Hv1^{-/-}$mice. For all animal studies, the protocols were approved by the Institutional Animal Care and Use Committee of Tongji Medical College, Huazhong University of Science and Technology (Wuhan, China) and Rutgers University (New Brunswick, NJ). Photothrombosis ischemia was performed in mice under anesthesia by inhalation of 3.5% isoflurane and maintained by inhalation of 1.0–2.0% isoflurane in 70% $N_2$ and 30% $O_2$ by a facemask. Body temperature was maintained at 37.0 ± 0.5 °C using a heating blanket. For the photothrombosis surgical procedure, bregma and lambda points were identified after a middle scalp incision, and then fiber optic bundle of a cold light source (KL1500 LCD, Carl Zeiss, Gottingen, Germany) with a 4 mm aperture was centered using a micromanipulator at 2mm right lateral to the bregma. A photosensitive dye rose Bengal (Sigma–Aldrich) was dissolved in sterile saline at a concentration of 10 mg/ml, and 1 mg of Rose Bengal in 0.1 ml was injected intraperitoneally (i.p) 5 min before illumination. The brain was illuminated through the intact skull for 15 min.

### Assessment of Neurological Deficit and Infarct Volumes

Neurological deficit assessment was performed on day 1 and 3 after stroke by investigators blinded to the wild type and Hv1 KO groups, these tests included the cylinder test, the hanging wire test, the pole test, and the rotarod test, as previously described (Brooks and Dunnett 2009; Li *et al.* 2014). For all the above-mentioned tests pre-training was done before ischemia.

After neurologic assessment, MR imaging was performed and the coronal brain images were obtained in DICOM format, and then were processed with Image J software. Infarct volumes were calculated by summation of the lesion areas of all slices and integrated by slice thickness (0.8 mm) with correction for brain swelling by the ratio of the ipsilateral volume to contralateral hemisphere (CH) volume from T2 weighted images ($T_2$WIs) (Pialat *et al.* 2007).

### Primary Microglial Cultures

Primary microglial cells were isolated from neonatal (1–3 days old) C57BL/6 wild type and $Hv1^{-/-}$ mice, as previously described (Hanisch *et al.* 1997). Briefly, cerebral cortices were isolated, meninges were removed, and tissue was minced in the presence of DNAse I (50 μg/ml, Sigma). Dissociated cells were passed through a 100μm pore mesh, pelleted at 1500 rpm for 5 min, and resuspended in culture medium. Cells were cultured in Dulbecco's modified Eagle's medium (DMEM) (Gibco) containing 10% FBS (Gibco), 1% penicilln-streptomycin (Gibco), 25 ng/ml mGM-CSF (R&D Systems). Media was replaced every 5 days. At approximately 14 and 21 days microglia were harvested by rapid shaking for 30

minutes. The purity of the microglia was > 95% as determined by CD11b and ionized calcium-binding adapter molecule 1 (Iba1) antibody. Isolated microglia cells were cultured for 24 hours in DMEM+1% penicillin-streptomycin followed by treatment with lipopolysaccharide (LPS, 100ng/ml) + interferon (IFN, 20ng/ml)-γ or interleukin-4 (IL-4, 20ng/ml) for 4h to promote polarization into the M1 or M2 phenotype, respectively.

### Immunohistochemistry

Three days after ischemia, animals were perfused with 4% paraformaldehyde in 0.1M phosphate buffer. Brain tissues were postfixed for 4–6h and immersed in gradient sucrose solutions for 24–48h at 4°C until they sank. Sections were cut (20μm thickness) with a cryostat and prepared for imunostaining. The slides were blocked with 1% bovine serum albumin containing 0.3% Triton X-100 for 1h. Sections were then incubated (overnight at 4°C) with the following primary antibodies: rabbit anti mouse Iba1 (1:500; Wako), goat anti mouse Arg1 (1:100; Santa Cruz), rabbit anti mouse iNOS (1:200; Abcam), mouse anti-8 hydroxyguanosine (8-OHG, Abcam, 1:200), mouse anti-NeuN (1:500, Chemicon), rabbit anti-Caspase 3(1:200, Abcam). The sections were then incubated (for 1h at room temperature) with the respective secondary fluorescent antibodies (all 1:500; Jackson ImmunoResearch) to visualize the primary antibodies. Images were acquired with a confocal microscope (Olympus).

### BrdU Incorporation and Detection

To identify the proliferation of microglia after ischemia, mice were injected with 200mg/kg bromodeoxyuridine (BrdU; Sigma) i.p. at 4 and 2h before being sacrificed for the experiments. Brain sections from BrdU-injected mice were treated to permeabilize the tissue and denature the DNA, and were then incubated overnight with the following primary antibodies: rabbit anti mouse Iba1 (1:500; Wako) and mouse monoclonal anti-BrdU antibody (1:50). The secondary antibodies (1: 500 dilutions) used were Alexa 488-labeled goat anti-mouse antibodies for BrdU detection and Alexa 594-labeled goat anti-rabbit antibodies for Iba-1 detection. For BrdU counting, three coronal sections per animal were analyzed with five randomly selected images within each area of interest (ischemic boundary zone). The total numbers of all $BrdU^+$ cells and $BrdU^+$ $iba1^+$ cells per field were counted.

### Western Blotting

Samples from brain tissues and cultured cells were lysed with lysis buffer (200 mM Tris [pH8.0], 150 mM NaCl, 2 mM EDTA, 1 mM NaF, 1% NP40, 1 mM PMSF and Protease inhibitor cocktail). The total protein concentration in the lysates was determined using the Bradford protein assay and 30 μg of protein from each sample was separated by 12% SDS-polyacrylamide gel electrophoresis and then transferred to a PVDF membrane. After transfer, the membranes were incubated with 5% skim milk in TBST for 1 h, followed by incubation overnight at 4°C with the primary antibodies, including CD16, iNOS, CD206, Arg1, β-actin. The blots were washed and incubated with appropriate HRP-conjugated secondary antibodies (Santa Cruz) for 1 h. All bands were detected using an ECL detection kit (Pierce Biotech, Rockford, IL, USA), and imaged using an Image Quant LAS-4000

image system (GE healthcare Life Science, Uppsala, Sweden). Results of Western blot assay are representative of at least three experiments.

### Quantifications and Statistical Analysis

All cell counts and intensity analysis were performed blind to the experimental treatment and data were expressed as mean±SEM. All statistical tests were performed using GraphPad Prism (GraphPad software, La Jolla, CA, USA). The group comparison was performed with Student-Newman-Keuls method (ANOVA) and then two-tailed t-test. $P < 0.05$ was considered to be statistically significant.

## Results

### Hv1 deficiency decreases infarct size and ameliorates neurological deficits after photothrombotic infarction

To observe the effects of Hv1 deficiency on ischemic stroke damage induced by photothrombosis, 3T MRI was used to assess the infarct size. The infarct lesion showed hyperintense signal intensity on T2- weighted images (Fig 1A). We measured infarct volume induced by photothrombosis and observed that infarction increased from acute phase at day 1 and remains persistent in sub-acute phase at day 3 post ischemia. In line with previous reports that deletion of Hv1 ameliorated ischemic stroke damage induced by middle cerebral artery occlusion (Wu *et al.* 2012), we found that the infarct volume in $Hv1^{-/-}$ mice was significantly smaller than that in wild-type mice at days 1 and 3, respectively after photothrombotic ischemia ($P<0.05$; Fig 1A).

Accompanied by a reduction in infarct size after ischemic stroke, neurological deficits measured by the rotarod test, the hanging wire test, the pole test and the cylinder test were significantly improved by Hv1 deletion compared to wild-type group, especially at day 3 post stroke (Fig 1B).

### Hv1 deficiency decreases neuronal cell death after photothrombosis

To further confirm the possible neuroprotective function of Hv1 deficiency during ischemic brain damage, we stained caspase-3 positive neurons in brain slices from mice after phtothrombosis. By using double immunofluorescence staining, we found that caspase-$3^{+}$ cells were largely accumulated in the infarct and peri-infarct areas, mainly colocalized with neuronal marker NeuN, indicating apoptotic neuronal cells after ischemia (Fig2). Consistent with the reduced infarction, the number of caspase-3-positive neurons was also decreased after photothorombosis in $Hv1^{-/-}$ mice compared to the mice in wild-type group ($P< 0.01$; Fig2). These results suggest that photothrombotic-induced ischemic neuronal damage was attenuated by Hv1 deletion.

### Hv1 deficiency decreases ROS production and but did not affect microglial proliferation after photothrombosis

Hv1 proton channel plays an important role in NOX-dependent ROS production in microglia (Wu 2014b; Wu *et al.* 2012). To characterize ROS production after photothromobotic ischemic stroke, we used an 8-OHG antibody to detect oxidized nucleic acids resulting from

cellular ROS damage (Nunomura *et al.* 1999). Three days after photothrombosis, the intensity of 8-OHG immunoreactive signals increased significantly in the boundary zone of infarct core compared with that in sham group (Fig. 3A, data was not shown in control). The 8-OHG signals were mainly localized in Iba-1$^{+}$ microglial cells indicating that microglia are the major ROS-producing cells after photothromobotic ischemia. In Hv1$^{-/-}$ mice, we found that the intensity of 8-OHG immunoreactive signals and the co-localization of 8-OHG signal and microglia were substantially reduced compared with wild type mice after ischemia (Fig. 3A). These results suggested that microglial Hv1 proton channels indeed contributed to microglial ROS production after photothrombotic ischemic brain damage.

To address whether the reduction in ROS production was due to the decreased number of microglial cells, we wanted to evaluate the impact of Hv1 proton channel deficiency on the proliferation of microglial cells after photothrombosis. To this end, Iba-1 immunostaining was performed to identify microglia and BrdU incorporation was used to study cell proliferation in the boundary zone of ischemic core. Consistent with previous studies (Patel *et al.* 2013; Li *et al.* 2014), the number of proliferating microglia, as measured by BrdU labeling, was largely increased at day 3 post ischemia in wild type mice (Fig. 3B). Interestingly, we found that there was no significant difference of the increased number of total BrdU$^{+}$ cells as well as Iba-1$^{+}$BrdU$^{+}$ double positive cells between in Hv1$^{-/-}$ mice and in wild type mice (Fig. 3C, $p > 0.05$). Together, these results indicated that Hv1 deficiency reduces photothrombosis-induced ROS production, but the reduction was not attributable to the microglial proliferation.

## Hv1 deficiency shifts microglia from M1 to M2 polarization state after photothrombotic ischemia and in cultured microglia

It has been reported that the suppression of ROS production shifts the microglial polarization from M1 toward M2 state, and attenuates brain injury after stroke (Choi *et al.* 2012); furthermore, NOX2 inhibition also could alter microglial polarization states (Khayrullina *et al.* 2015b). As Hv1 proton channel was required for NOX-dependent ROS generation in the brain, we speculated that Hv1 might be a potential target for modulating microglial M1/M2 polarization during the pathological process of ischemic brain damage. To examine the effect of Hv1 deficiency after ischemic stroke on M1/M2 microglial polarity, we assessed polarization markers in the brain after photothrombotic ischemia using immunohistochemistry and western blotting. The expression of M1 markers, including iNOS and CD16, was significantly increased after photothrombosis compared to that in the sham group. However, these increases were markedly attenuated in the Hv1$^{-/-}$ mice after stroke compared to wild type group ($p < 0.01$) (Fig. 4). Similarly, the expression of M2 markers CD206 and arginase was up-regulated in the wild type group after injury; but the increase of M2 maker was significant in Hv1$^{-/-}$ group in comparison to the wild type group (Fig. 4).

The M1/M2 markers, including iNOS, CD16, CD206 and arginase, are not specific for microglia, which also can be produced by other cells like neurons and astrocytes. It cannot be concluded simply that M1/M2 microglial polarization was modulated by Hv1 proton channel based on the Western blot results. To circumvent this issue, we used immunostaining to examine the colocalization of characteristic M1/M2 polarization marker

with microglial maker Iba-1. Consistent with the Western blot results, the expression of the M1 marker iNOS was highly presented in $Iba1^+$ cells in ischemic mouse brain slices. The co-expression was obviously less in the deletion of Hv1 mice (Fig. 5A,C). In contrast, the co-expression of M2 marker arginase and Iba1 was higher in the $Hv1^{-/-}$ group post photothrombosis compared with the wild type group (Fig. 5B,C). Together, our Western blot and immunostaining results consistently indicated that Hv1 proton channel might regulate microglial polarization states, likely due to its function in NOX inhibition.

To further investigate the function of Hv1 proton channel in regulating microglial polarity, we used primary cultured microglia and directly induced M1/M2 polarization *in vitro*. The expression of M1 markers (iNOS and CD16) was significantly increased by LPS plus IFN-γ stimulation. Indeed, we found that this upregulation of iNOS and CD16 was attenuated by Hv1 deficiency (Fig. 6A,B). On the other hand, the expression of M2 markers (arginase1 and CD206) in cultured microglia from wild type group was upregulated when stimulated by IL-4. Interestingly, we found that Hv1 deficiency increased the expression of M2 markers compared to that in wild type group (Fig. 6C,D).

## Discussion

In the current study, we demonstrate that microglial Hv1 contributed substantially to neuronal damage and neurological dysfunction in the pathological process after photothrombosis of cortical microvessels. Hv1 deficiency led to significant improvements in a number of measures of recovery in this experimental ischemia. The rescue of ischemic brain damage by Hv1 deficiency was seen on both the functional and cellular levels. First, infarct size was substantially reduced in $Hv1^{-/-}$ mice compared with wild type mice after ischemia. Second, neurological dysfunction after ischemia was reduced in $Hv1^{-/-}$ mice. The functional improvement observed was measured using holding wire test, rotarod test, cylinder test and pole test, suggesting improvements in both gross and fine motor skills. Third, reduced neuronal apoptosis was observed in $Hv1^{-/-}$ mice compared with wild type mice after photothrombosis, and thus microglial Hv1 was likely responsible for neuronal damage at the acute stage following ischemia.

Microglia and macrophages are among the first cells to respond to CNS injuries and are potent modulators of CNS repair and regeneration (Hu *et al.* 2014; Davalos *et al.* 2005). Traditionally, these cells are considered to hinder CNS repair and expand tissue damage by releasing destructive pro-inflammatory mediators, and inhibition of microglia activation can attenuate ischemia induced brain injury (Ma *et al.* 2016). However, our data showed that there's no significant reduction of $Brdu^+$ cells nor $Iba1^+Brdu^+$ cells in the peri-infarct region, so the protective effect of $Hv1^{-/-}$ in ischemia might not result from inhibition of microglial proliferation. Concurrently, a considerable body of literature suggests that activated microglia with distinct phenotypes are apparently double-edged swords in the battle for neurological recovery after stroke or other injuries (Hu *et al.* 2014; Kwon *et al.* 2013; Miron *et al.* 2013; Liu *et al.* 2007). Differential polarization of microglia could likely explain the biphasic role of microglia in brain ischemia.

Based on the stimulation of pro-inflammatory cytokines (like IFN-γ and LPS) or anti-inflammatory cytokines (like IL-4 and IL-13), microglia could generally polarize into M1 and M2 phenotypes both *in vitro* and *in vivo* (Gordon 2003). M1 phenotype is designated as classically activated microglia and characterized by enhanced expression of CD16/32, iNOS and production of a variety of pro-inflammatory cytokines (IL-1β, IL-6 and TNF-a), ROS, NO (Kettenmann *et al.* 2011; Saijo and Glass 2011). M2 phenotype could be induced by IL-4 or IL-13 stimulation and are mainly considered to suppress inflammation. Generally, M2 microglia display enhanced expression of Arginase-1, Ym1 and CD206 (Mecha *et al.* 2015; Latta *et al.* 2015), and is capable of producing anti-inflammatory cytokines IL-10, IL-4, IL-13 and IGF-1, as well as expressing scavenge receptors, contributing to inhibiting inflammation and promoting tissue repair (Cherry *et al.* 2014; Ponomarev *et al.* 2013). Among ion channels selectively expressed in microglia, the voltage-gated proton channel HV1 is a recently cloned ion channel that rapidly removes protons from depolarized cytoplasm; Microglial HV1 regulates intracellular pH and aids in NADPH oxidase-dependent generation of ROS(Wu 2014b). ROS have an established role in inflammation, and pharmacological blockade of mitochondrial ROS efficiently reduces inflammatory cytokine production(Bulua *et al.* 2011). Whether Hv1 deficiency could modulate microglial polarization in ischemic stroke remains unclear.

Here we provided a detailed description of Hv1 deficiency on microglial polarization *in vivo* after photothrombotic ischemia or *in vitro* in cultured microglia. It was demonstrated that there is a balance of M1 and M2 markers acutely after ischemia that is followed by an increase in the M1:M2 ratio in the acute period (Kigerl *et al.* 2009). Our data support the idea that there's elevated M1 and M2 marker expression and a shift toward M1 dominance at acute time points post-ischemia. Hv1 deficiency appears to limit this shift. In $Hv1^{-/-}$ mice, the expression of M2 markers (Arg1 and CD206) were enhanced over time, while M1 related markers (iNOS and CD16/32) were reduced from the 1st day after ischemia, compared with the wild type mice. These results indicated that Hv1 deficiency *in vivo* not only reduced the inflammatory response of microglia, but also rather pushed it toward a more protective phenotype.

Consistently, in cultured microglia, we have shown that Hv1 deficiency can influence acute alterations in microglial polarization. Administration of the M1-polarizing cytokines LPS and IFN-γ induced an enhanced expression of M1 markers like iNOS and CD16/32. Inhibition of Hv1 activity, via knockout of Hv1, significantly reduced M1 polarization and shifted LPS-treated microglia to an M2 polarization state. When treated with M2-polarizing cytokine IL-4, on the other hand, Hv1 deficiency promoted microglia polarization toward M2 phenotype by enhancing anti-inflammatory markers like CD206 and arginase-1. This shift was usually accompanied by a reduction in pro-inflammatory cytokines and may create a favorable microenvironment for CNS repair as reported previously (Khayrullina *et al.* 2015a).

Hv1 proton channel was reported to contribute substantially to NOX ROS production, supporting NOX-mediated neuronal cell death after stroke and cuprizone-induced demyelination (Wu *et al.* 2012; Liu *et al.* 2015). Concurrently, superoxide synthesis is an important inducer of M1 macrophage/microglia differentiation. For instance, in the absence

of NOX-derived superoxide, macrophages exhibit an alternatively activated M2 phenotype during Type1 Diabetes (Padgett *et al.* 2015). Further exploration proved that inhibition of NOX specifically reduces M1 polarization, increases M2 polarization, reduces a number of pro-inflammatory markers and consequently improves outcome after neuronal injury in central nervous system (Khayrullina *et al.* 2015a). Our data indicate that Hv1 deficiency attenuate brain damage via skewing the balance of the microglial response toward protection and regenerative processes during ischemia. This protective effect is probably related to Hv1's role in NOX activation. However, we cannot exclude the possibility that Hv1 regulation of intracellular pH may participate in the switch of microglial M1/M2 polarization(Wu 2014a). Future studies will determine how Hv1 related ROS modulates microglia polarization, and whether there is underlined pathways other than ROS that may be involved. Nevertheless, our study provides a novel insight on the function of Hv1 proton channel in microglial polarity. Therefore, Hv1 inhibition is a potential therapeutic strategy to promote an alternatively activated M2 phenotype of microglia, which may be beneficial in the treatment of ischemic stroke.

## Acknowledgments

This work is supported by National Natural Science Foundation of China (NSFC, 81101766, 81171157, 81571132) and National Institute of Health (R01NS088627, R21DE025689). All experiments were conducted in compliance with the ARRIVE guidelines.

## Abbreviations

| | |
|---|---|
| **NOX** | NADPH oxidase |
| **ROS** | reactive oxygen species |
| **DMEM** | Dulbecco's modified Eagle's medium |
| **Iba1** | ionized calcium-binding adapter molecule 1 |
| **LPS** | lipopolysaccharide |
| **IFN** | interferon |
| **IL-4** | interleukin-4 |
| **8-OHG** | 8-hydroxy guanosine |
| **BrdU** | bromodeoxyuridine |

## Reference

Brooks SP, Dunnett SB. Tests to assess motor phenotype in mice: a user's guide. Nat. Rev. Neurosci. 2009; 10:519–529. [PubMed: 19513088]

Bulua AC, Simon A, Maddipati R, Pelletier M, Park H, Kim K-Y, Sack MN, Kastner DL, Siegel RM. Mitochondrial reactive oxygen species promote production of proinflammatory cytokines and are elevated in TNFR1-associated periodic syndrome. J. Exp. Med. 2011; TRAPS; 208:519–533. [PubMed: 21282379]

Cherry JD, Olschowka JA, O'Banion MK. Neuroinflammation and M2 microglia: the good, the bad, and the inflamed. Journal of Neuroinflammation. 2014; 11:98. [PubMed: 24889886]

Choi S-H, Aid S, Kim H-W, Jackson SH, Bosetti F. Inhibition of NADPH oxidase promotes alternative and anti-inflammatory microglial activation during neuroinflammation. Journal of Neurochemistry. 2012; 120:292–301. [PubMed: 22050439]

Cooney SJ, Bermudez-Sabogal SL, Byrnes KR. Cellular and temporal expression of NADPH oxidase (NOX) isotypes after brain injury. Journal of Neuroinflammation. 2013; 10:155. [PubMed: 24344836]

Davalos D, Grutzendler J, Yang G, Kim JV, Zuo Y, Jung S, Littman DR, Dustin ML, Gan W-B. ATP mediates rapid microglial response to local brain injury in vivo. Nat Neurosci. 2005; 8:752–758. [PubMed: 15895084]

Gordon S. Alternative activation of macrophages. Nat. Rev. Immunol. 2003; 3:23–35. [PubMed: 12511873]

Hanisch UK, Lyons SA, Prinz M, Nolte C, Weber JR, Kettenmann H, Kirchhoff F. Mouse brain microglia express interleukin-15 and its multimeric receptor complex functionally coupled to Janus kinase activity. J. Biol. Chem. 1997; 272:28853–28860. [PubMed: 9360952]

Hu X, Leak RK, Shi Y, Suenaga J, Gao Y, Zheng P, Chen J. Microglial and macrophage polarization—new prospects for brain repair. 2014:1–9.

Hu X, Li P, Guo Y, Wang H, Leak RK, Chen S, Gao Y, Chen J. Microglia/Macrophage Polarization Dynamics Reveal Novel Mechanism of Injury Expansion After Focal Cerebral Ischemia. Stroke. 2012; 43:3063–3070. [PubMed: 22933588]

Hur J, Lee P, Kim MJ, Kim Y, Cho Y-W. Ischemia-activated microglia induces neuronal injury via activation of gp91phox NADPH oxidase. Biochem. Biophys. Res. Commun. 2010; 391:1526–1530. [PubMed: 20036216]

Kahles T, Kohnen A, Heumueller S, Rappert A, Bechmann I, Liebner S, Wittko IM, et al. NADPH oxidase Nox1 contributes to ischemic injury in experimental stroke in mice. Neurobiol. Dis. 2010; 40:185–192. [PubMed: 20580928]

Kahles T, Luedike P, Endres M, Galla H-J, Steinmetz H, Busse R, Neumann-Haefelin T, Brandes RP. NADPH oxidase plays a central role in blood-brain barrier damage in experimental stroke. Stroke. 2007; 38:3000–3006. [PubMed: 17916764]

Kettenmann H, Hanisch U-K, Noda M, Verkhratsky A. Physiology of microglia. Physiol. Rev. 2011; 91:461–553. [PubMed: 21527731]

Khayrullina G, Bermudez S, Byrnes KR. Inhibition of NOX2 reduces locomotor impairment, inflammation, and oxidative stress after spinal cord injury. Journal of Neuroinflammation. 2015a: 1–11.

Khayrullina G, Bermudez S, Byrnes KR. Inhibition of NOX2 reduces locomotor impairment, inflammation, and oxidative stress after spinal cord injury. Journal of Neuroinflammation. 2015b; 12:3249–11.

Kigerl KA, Gensel JC, Ankeny DP, Alexander JK, Donnelly DJ, Popovich PG. Identification of two distinct macrophage subsets with divergent effects causing either neurotoxicity or regeneration in the injured mouse spinal cord. J. Neurosci. 2009; 29:13435–13444. [PubMed: 19864556]

Kumar A, Alvarez-Croda D-M, Stoica BA, Faden AI, Loane DJ. Microglial/Macrophage Polarization Dynamics following Traumatic Brain Injury. J. Neurotrauma. 2015 neu.2015.4268.

Kwon MJ, Kim J, Shin H, Jeong SR, Kang YM, Choi JY, Hwang DH, Kim BG. Contribution of macrophages to enhanced regenerative capacity of dorsal root ganglia sensory neurons by conditioning injury. J. Neurosci. 2013; 33:15095–15108. [PubMed: 24048840]

Latta CH, Sudduth TL, Weekman EM, Brothers HM, Abner EL, Popa GJ, Mendenhall MD, Gonzalez-Oregon F, Braun K, Wilcock DM. Determining the role of IL-4 induced neuroinflammation in microglial activity and amyloid-β using BV2 microglial cells and APP/PS1 transgenic mice. Journal of Neuroinflammation. 2015; 12:41. [PubMed: 25885682]

Li H, Zhang N, Lin H-Y, Yu Y, Cai Q-Y, Ma L, Ding S. Histological, cellular and behavioral assessments of stroke outcomes after photothrombosis-induced ischemia in adult mice. BMC Neurosci. 2014; 15:58. [PubMed: 24886391]

Liu J, Tian D, Murugan M, Eyo UB, Dreyfus CF, Wang W, Wu L-J. Microglial Hv1 proton channel promotes cuprizone-induced demyelination through oxidative damage. Journal of Neurochemistry. 2015; 135:347–356. [PubMed: 26173779]

Liu Z, Fan Y, Won SJ, Neumann M, Hu D, Zhou L, Weinstein PR, Liu J. Chronic treatment with minocycline preserves adult new neurons and reduces functional impairment after focal cerebral ischemia. Stroke. 2007; 38:146–152. [PubMed: 17122429]

Ma Y, Wang J, Wang Y, Yang G-Y. The biphasic function of microglia in ischemic stroke. Progress in Neurobiology. 2016

Mecha M, Feliú A, Carrillo-Salinas FJ, Rueda-Zubiaurre A, Ortega-Gutiérrez S, de Sola RG, Guaza C. Endocannabinoids drive the acquisition of an alternative phenotype in microglia. Brain Behav. Immun. 2015; 49:233–245. [PubMed: 26086345]

Miller E, Wachowicz B, Majsterek I. Advances in antioxidative therapy of multiple sclerosis. Curr. Med. Chem. 2013; 20:4720–4730. [PubMed: 23834174]

Miron VE, Boyd A, Zhao J-W, Yuen TJ, Ruckh JM, Shadrach JL, van Wijngaarden P, et al. M2 microglia and macrophages drive oligodendrocyte differentiation during CNS remyelination. Nat Neurosci. 2013; 16:1211–1218. [PubMed: 23872599]

Nunomura A, Perry G, Pappolla MA, Wade R, Hirai K, Chiba S, Smith MA. RNA oxidation is a prominent feature of vulnerable neurons in Alzheimer's disease. Journal of Neuroscience. 1999; 19:1959–1964. [PubMed: 10066249]

Padgett LE, Burg AR, Lei W, Tse HM. Loss of NADPH Oxidase–Derived Superoxide Skews Macrophage Phenotypes to Delay Type 1 Diabetes. Diabetes. 2015; 64:937–946. [PubMed: 25288672]

Patel AR, Ritzel R, McCullough LD, Liu F. Microglia and ischemic stroke: a double-edged sword. Int J Physiol Pathophysiol Pharmacol. 2013; 5:73–90. [PubMed: 23750306]

Pialat J-B, Cho T-H, Beuf O, Joye E, Moucharrafie S, Moucharaffie S, Langlois J-B, et al. MRI monitoring of focal cerebral ischemia in peroxisome proliferator-activated receptor (PPAR)-deficient mice. NMR Biomed. 2007; 20:335–342. [PubMed: 17451173]

Ponomarev ED, Veremeyko T, Weiner HL. MicroRNAs are universal regulators of differentiation, activation, and polarization of microglia and macrophages in normal and diseased CNS. Glia. 2013; 61:91–103. [PubMed: 22653784]

Ramsey IS, Moran MM, Chong JA, Clapham DE. A voltage-gated proton-selective channel lacking the pore domain. Nature. 2006; 440:1213–1216. [PubMed: 16554753]

Saijo K, Glass CK. Microglial cell origin and phenotypes in health and disease. Nat. Rev. Immunol. 2011; 11:775–787. [PubMed: 22025055]

Sasaki M, Takagi M, Okamura Y. A voltage sensor-domain protein is a voltage-gated proton channel. Science. 2006; 312:589–592. [PubMed: 16556803]

Taylor RA, Sansing LH. Microglial responses after ischemic stroke and intracerebral hemorrhage. Clin. Dev. Immunol. 2013; 2013:746068–10. [PubMed: 24223607]

Wu L-J. Microglial voltage-gated proton channel Hv1 in ischemic stroke. Transl Stroke Res. 2014a; 5:99–108. [PubMed: 24323712]

Wu L-J. Voltage-gated proton channel HV1 in microglia. Neuroscientist. 2014b; 20:599–609. [PubMed: 24463247]

Wu L-J, Wu G, Akhavan Sharif MR, Baker A, Jia Y, Fahey FH, Luo HR, Feener EP, Clapham DE. The voltage-gated proton channel Hv1 enhances brain damage from ischemic stroke. Nat Neurosci. 2012; 15:565–573. [PubMed: 22388960]

Yrjänheikki J, Keinänen R, Pellikka M, Hökfelt T, Koistinaho J. Tetracyclines inhibit microglial activation and are neuroprotective in global brain ischemia. Proc. Natl. Acad. Sci. U.S.A. 1998; 95:15769–15774. [PubMed: 9861045]

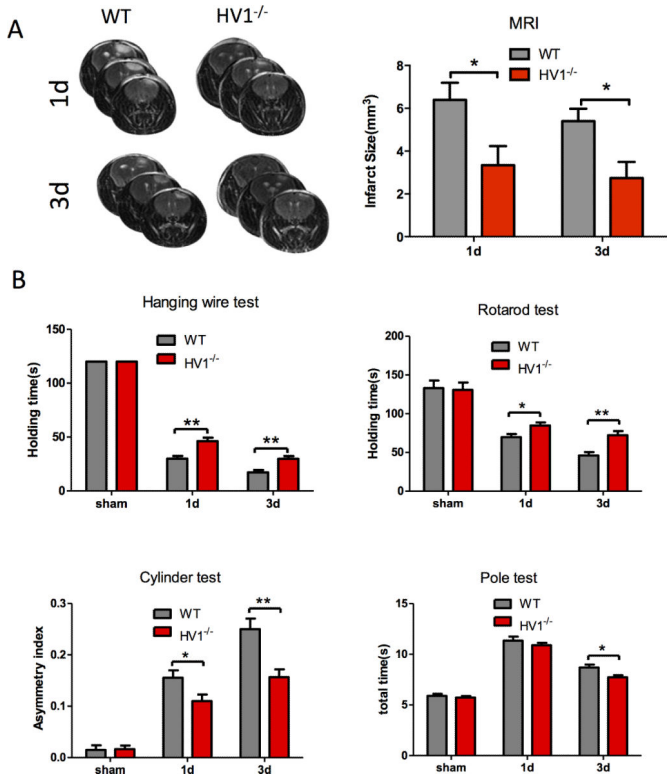


**Fig.1. Hv1 deficiency reduces infarct size and ameliorates neurological outcome at day 1 and 3 after photothrombotic stroke**

Representative brain MRI images of infarction at day 1 and 3 after stroke were shown in Fig1A (left panel). Quantitative and statistical analysis of infarct size data was presented in the right panel of Fig1A. Measurement by MRI revealed a significant reduction in infarction size in $Hv1^{-/-}$ mice compared to wild type mice. Data are mean ± SEM; $*p < 0.05$. Neurological deficits measured by the rotarod test, the hanging wire test, the pole test and the cylinder test revealed a better outcome in $Hv1^{-/-}$ mice compared to wild type mice at day 1 and 3 post stroke, especially after 3 days (Fig 1B). Data are mean ± SEM; $*p < 0.05$, $**p < 0.01$.

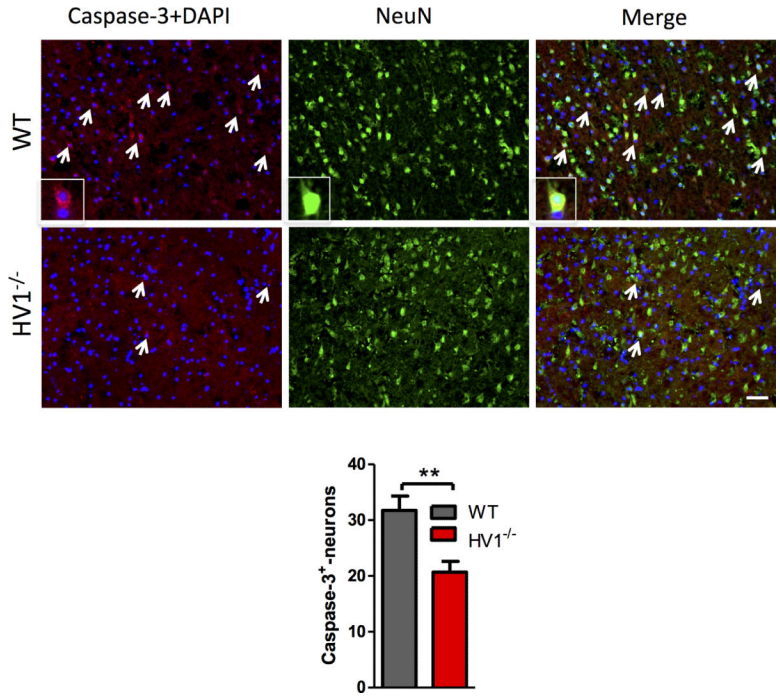


**Fig.2. Hv1 deficiency decreases neuronal apoptosis after photothrombotic stroke**

Triple-staining for caspase-3 (red fluorescence), neuronal nuclear marker NeuN (green fluorescence), and nuclear staining (DAPI, blue) showed expression of neuronal apoptosis in the boundary zone of infarct core (arrows). Quantification of caspase-$3^+$ neurons in the ischemic area showed the fewer number of apoptotic neuronal cells in $Hv1^{-/-}$ group as compared with the wild type group; Data are mean ± SEM; $^{**}p < 0.01$.

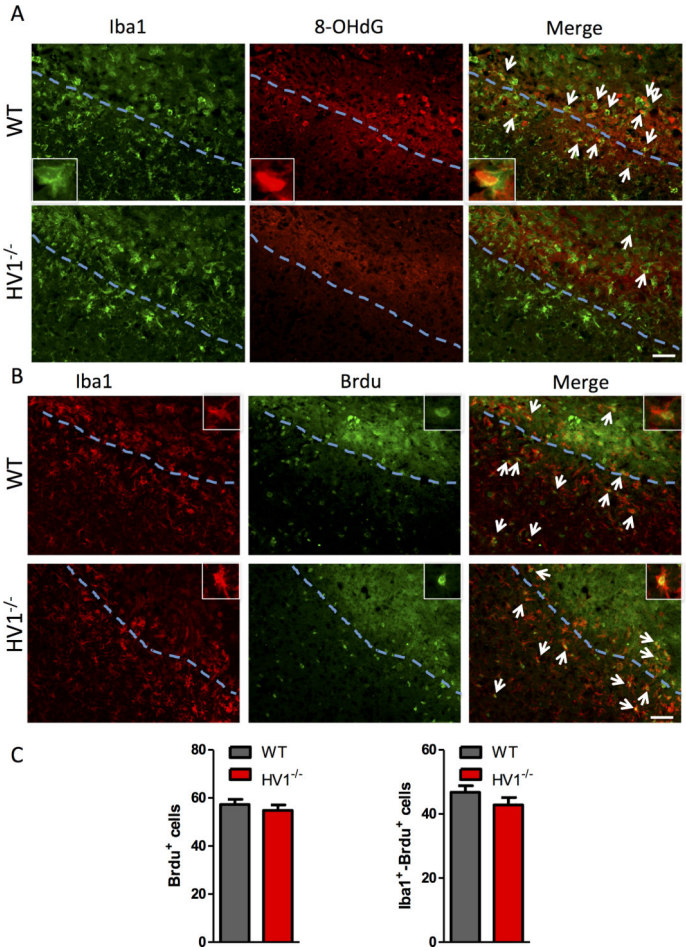


**Fig.3. Hv1 deficiency inhibited microglial ROS production after ischemic stroke**

(A) Representative images showing microglial ROS production examined by 8 hydroxyguanosine (8-OHG) and microglia marker Iba-1 double immunostaining (arrows). 8-OHG immunoreactivity was dramatically increased and microglia was significantly activated in the brain ischemic zone after day 3. However, the stroke-induced increase in 8-OHG staining was attenuated in $Hv1^{-/-}$mice compared with wild type mice. Insets are the magnified images shown for a single microglia that is 8-OHG positive. Dotted blue line delineated the boundary ischemic zone for the analysis of immunostaining. Scale bar, 200 μm. (B) Representative images showing double staining of Iba-1 and bromodeoxyuridine (BrdU) in the boundary zone of either wild type or $Hv1^{-/-}$mice. Arrows point to $BrdU^+$ $Iba\text{-}1^+$ cells. Insets are respective enlarged images of $BrdU^+$ $Iba\text{-}1^+$ cells. Scale bar, 200 μm. (C) The summarized bar graphs showing the number of $BrdU^+$ cells (left) and $BrdU^+Iba\text{-}1^+$ cells (right) in the ischemic region in wild type and $Hv1^{-/-}$mice (n = 4 mice in each group).

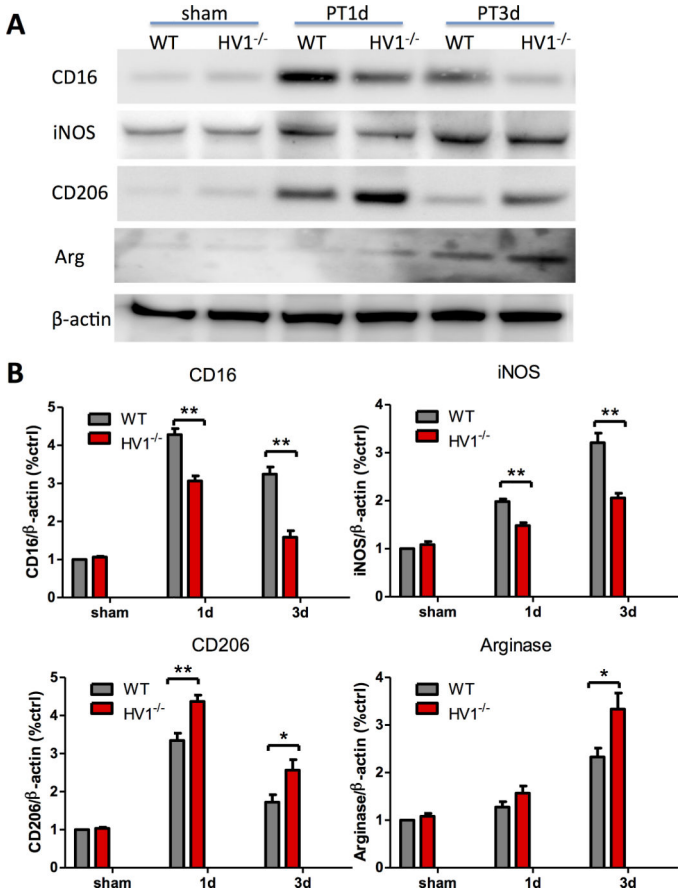


**Fig.4. Hv1 deficiency decreased the production of M1/M2 markers after ischemic stroke**

(A) Representative Western blots images of microglial M1/M2 markers in the ischemic boundary zone at day 3 post stroke from sham control and ischemic wild type and $Hv1^{-/-}$mice. CD16 and iNOS for M1 markers; Arginase and CD206 for M2 markers. (B) Summarized data showing that microglial M1 marker (CD16 and iNOS) increase was compromised in $Hv1^{-/-}$mice compared with that in wild type mice. In addtion, Hv1 deficiency up-regulated the expression of M2 marker after ischemic stroke compared to the wild type group. Each bar is shown as a ratio of its own optical density to that of beta-actin expression (n = 4 mice for each group). *$p < 0.05$, **$p < 0.01$.

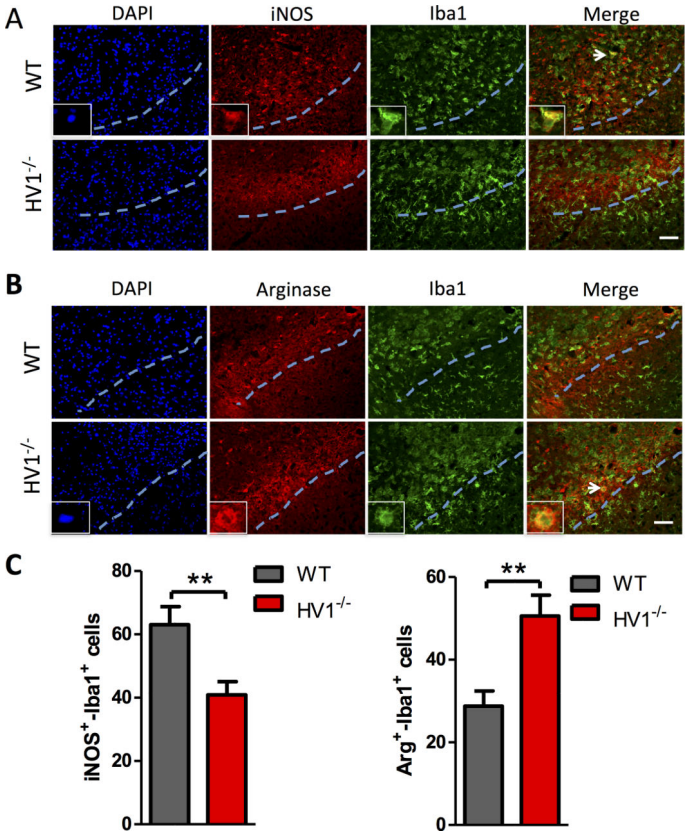


**Fig.5. Hv1 deficiency modulates microglial M1/M2 polarization state after ischemic stroke**

Representative images showing microglial M1/M2 polarization examined by iNOS (M1), Arg1 (M2) and microglia marker Iba-1 double immunostaining (arrows). Dotted blue line delineated the ischemic boundary zone for the analysis of immunostaining. (A) iNOS was dramatically increased and microglia was significantly activated in the brain ischemic zone after day 3. However, the stroke-induced increase in iNOS staining was attenuated in $Hv1^{-/-}$ mice compared with wild type mice. Insets are the magnified images shown for a single microglia that is iNOS positive. (B) Arginase immunoreactivity was dramatically increased and mainly expressed in the Iba-$1^{+}$ microglia, located in the brain ischemic zone after day 3. Whereas, up-regulation of arginase immunoreactivity was more pronounced in $Hv1^{-/-}$ mice compared with wild type mice. Arrows point to $Arg1^{+}$ Iba-$1^{+}$ cells. Insets are respective enlarged images of $Arg1^{+}$ Iba-$1^{+}$ cells. Scale bar, 200 μm. (C) The summarized bar graphs showed that the number of $iNOS^{+}$ microglial cells (left) and $Arg1^{+}$ microglial cells (right) in the ischemic region in wild type and $Hv1^{-/-}$ mice (n = 4 mice in each group).

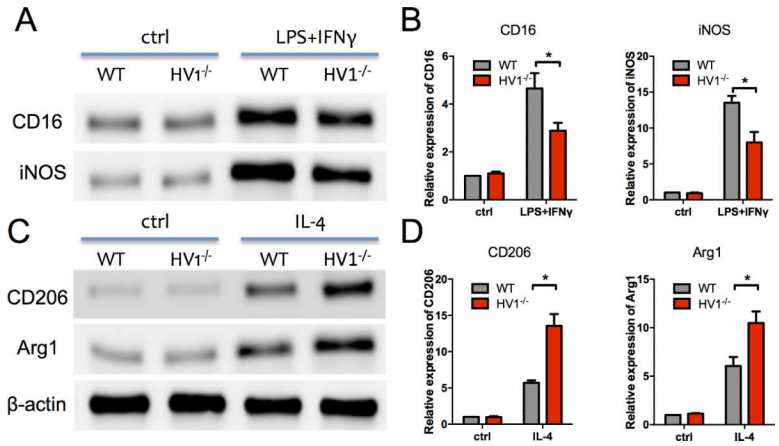


**Fig.6. Hv1 deficiency enhances M2 polarization of cultured microglia**

Representative images of Western blot for iNOS, CD16/32(M1 phenotype) (Fig.6A) and CD206, Arg1 (M2 phenotype) (Fig.6C) in primary microglial cells isolated from wild type and $HV1^{-/-}$mice. Cells were stimulated with lipopolysaccharide (LPS) + interferon (IFN)-γ or interleukin (IL)-4 for 24h. (B,D) Densitometric analysis of iNOS, CD16/32, CD206 and Arg1 normalized to β-actin/GAPDH. Hv1 deficiency significantly reduced the expression of the M1 markers, iNOS and CD16/32, and upregulated the expression of the M2 markers, Arg1 and CD206. $n = 4$ in each group. $^{*}p < 0.05$.